

## Preliminary study on ultrasonic visualization of myocardial contractile response based on local strain rate measurement

Yu Obara<sup>1‡</sup>, Shohei Mori<sup>2\*</sup>, Nobuo Masauzi<sup>1</sup>, Masumi Iwai-Takano<sup>3,4,5,1</sup>, Mototaka Arakawa<sup>1,2</sup>, and Hiroshi Kanai<sup>2,1</sup> (<sup>1</sup>Grad. Sch. Biomed. Eng., Tohoku Univ.; <sup>2</sup>Grad. Sch. Eng., Tohoku Univ.; <sup>3</sup>Sch. Pharm. Sci., Ohu Univ.; <sup>4</sup>Dept. Epidemiol., Fukushima Med. Univ.; <sup>5</sup>Dept. Cardiovasc. Surg., Fukushima Med. Univ.)

### 1. Introduction

Myocardial ischemia leads to an abnormality in the propagation of the contractile response to the electrical excitation of the myocardium.<sup>1)</sup> This contractile response can be captured by ultrasound measurements.<sup>1-3)</sup> The local visualization of the contractile response may contribute to the detection of myocardial ischemia.

In our previous study for healthy volunteers, the propagation of the contractile response in the left ventricular (LV) wall was locally captured by the local strain rate (SR) measurement.<sup>4)</sup> In the local measurement, the contractile response was observed to propagate along the longitudinal direction of the LV wall and different for depth within the LV wall.

In the present paper, the propagation of the contractile response was visualized based on the waveforms of the SR locally measured. The difference in the propagations between the right ventricular (RV) and LV sides was discussed.

### 2. Methods

*In vivo* measurement was applied to the interventricular septum (IVS) of a 26-year-old healthy man in the parasternal long-axis view, as shown in **Fig. 1(a)**. The RF signal was obtained by the ultrasound diagnostic apparatus (F75, Aloka) with a sector probe of the 3-MHz center frequency and the 20-MHz sampling frequency. The frame rate was set at 503 Hz and the focused beams in different ten directions at the steering angles of 5.6° intervals were transmitted for each frame. The spatial resolution of the received beam (full width of half the maximum) in the lateral direction was 1.8 mm.

The electrocardiogram (ECG) and phonocardiogram (PCG) waveforms were acquired using three electrodes and a small accelerometer attached to the subject's chest, respectively.

The SR was locally measured around the time phase of the ECG R-wave when the electrical excitation conducts through the LV wall. The velocity of the myocardium was locally estimated using the multifrequency phased-tracking method with the ±1.25 mm of Tukey window (taper ratio: 0.3) at multiple points in the IVS. The SR at the  $m$ th

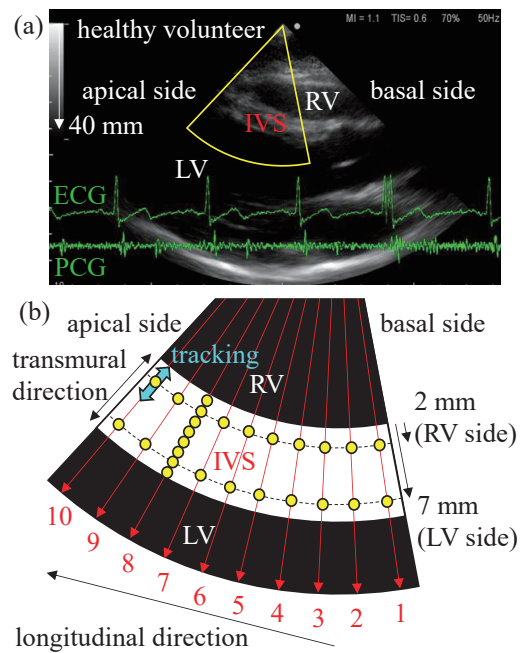


Fig. 1 (a) B-mode image, (b) interest points for obtaining the SR waveform.

beam of the  $i$ th frame was calculated using the estimated velocities  $\hat{v}_{i,m}$  as follows.

$$\widehat{SR}_{i,m}(n) = \frac{\hat{v}_{i,m}\left(n + \frac{h}{2}\right) - \hat{v}_{i,m}\left(n - \frac{h}{2}\right)}{G_{i,m}\left(n + \frac{h}{2}\right) - G_{i,m}\left(n - \frac{h}{2}\right)}. \quad (1)$$

Here,  $n$  is the sample depth,  $h$  is the sample interval for calculating SR, and  $G_{i,m}$  is the effective depth of the velocity estimation window. The spatial interval for calculating SR was set at 1 mm ( $h = 26$ ).  $G_{i,m}$  was obtained by calculating the depth of the center of gravity of the RF envelopes.<sup>5)</sup>

The SR waveform was obtained based on the estimated SR at the interest point tracked by integrating the estimated velocity. As shown in **Fig. 1(b)**, the interest points were set at depths of 2 mm (RV side) and 7 mm (LV side) from the surface of the RV side for each beam. In the 8th beam, the multiple interest points were set in the transmural direction of the IVS. The first zero-crossing from negative to positive of the SR waveform was detected as the contractile response within the ECG QR-interval because the thickness of the myocardium increases after the electrical excitation. The speed of propagation was obtained by the least squared method with the weight of the positive SR.

E-mail: <sup>‡</sup>yu.obara.s2@dc.tohoku.ac.jp, <sup>\*</sup>mori@tohoku.ac.jp

### 3. Results and Discussion

**Figure 2** shows the SR waveforms and the propagation of the contractile response in the transmural direction. In the SR waveform, the blue and red show the positive and negative SRs, respectively. The blue plus signs (+) show the detected contractile response. The times of the detected contractile response in the RV and LV sides were earlier than those in the mid of the IVS. The propagation of the contractile response across the IVS in the transmural direction was not observed.

**Figure 3** shows the SR waveforms and the propagation of the contractile response in the longitudinal direction. The blue arrow shows the estimated propagation of the contractile response. As shown in Fig. 3(b), the contractile response propagated from the basal to the apical side in the LV side. The estimated speed was 2.3 m/s. In the RV side, however, the time of the detected contractile response widely varied within the ECG QR-interval. The estimated speed in the RV side (0.4 m/s) was much lower than that in the LV side.

The difference in the propagations of the contractile response between the RV and LV sides might relate to the specialized myocardium of the left bundle branch (LBB). The speed of the electrical conduction through the specialized myocardium (1-5 m/s) is much faster than that through the myocardium in the longitudinal direction (0.07–0.7 m/s).<sup>6,7)</sup> The LBB runs from the basal side to the apical side in the longitudinal direction. The speed and direction of the propagation of the contractile response often correspond to the electrical conduction through the LBB. The propagation of the contractile response in the LV side in Fig. 3 might be affected by the electrical conduction through the LBB. That in the RV side in Fig. 3 might be related to the electrical conduction through the myocardium because the spread of the right bundle branch is less than that of the LBB.

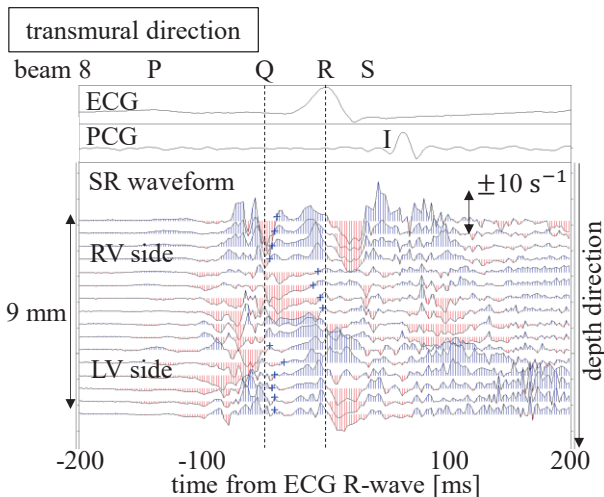


Fig. 2 SR waveforms and the propagation of the contractile response in the transmural direction.

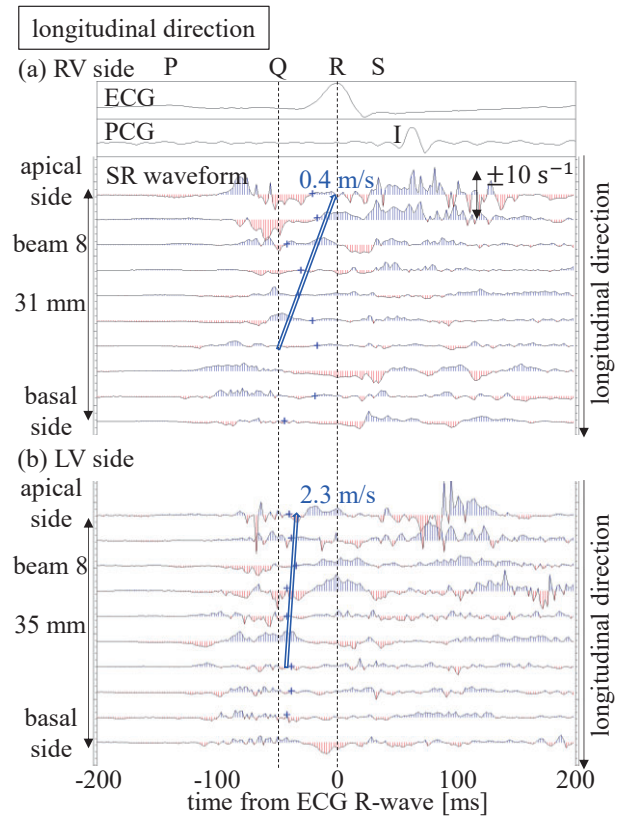


Fig. 3 SR waveforms and the propagation of the contractile response in the longitudinal direction. (a) RV side and (b) LV side.

### 4. Conclusion

The propagation of the contractile response based on the SR waveforms was different between the RV and LV sides. The local SR measurement may be useful to visualize these different propagations of the contractile response.

### Acknowledgment

This work was supported by JSPS KAKENHI 22KJ0227.

### References

- 1) Y. Matsuno, H. Taki, H. Yamamoto, M. Hirono, S. Morosawa, H. Shimokawa, and H. Kanai, *Jpn. J. Appl. Phys.* **56**, 07JF05 (2017).
- 2) Y. Honjo, H. Hasegawa, and H. Kanai, *Jpn. J. Appl. Phys.* **51**, 07GF06 (2012).
- 3) A. Hayashi, S. Mori, M. Arakawa, and H. Kanai, *Jpn. J. Appl. Phys.* **58**, SGGE05 (2019).
- 4) Y. Obara, S. Mori, M. Arakawa, and H. Kanai, *Jpn. J. Appl. Phys.* **60**, SDDE02 (2021).
- 5) Y. Obara, S. Mori, M. Iwai-Takano, M. Arakawa, and H. Kanai, *Proc. 43rd Symp. Ultrasonic Electronics*, 2022, 2Pa5-1.
- 6) T. Sano, N. Takayama, and T. Shimamoto, *Circ. Res.* **7**, 262 (1959).
- 7) A. M. Scher, A. C. Young, A. L. Malmgreen, and R. R. Paton, *Circ. Res.* **1**, 539 (1953).